Microwave and Millimeter Wave Nondestructive Evaluation of the Space Shuttle External Tank Insulating Foam

S. Shrestha[1], S. Kharkovsky[1], R. Zoughi[1] and F. Hepburn[2]

[1]*Applied Microwave Nondestructive Testing Laboratory (amntl)*
Electrical and Computer Engineering Department
University of Missouri-Rolla
Rolla, Missouri 65409

[2]*NASA George C. Marshall Space Flight Center*
Marshall Space Flight Center, AL 35812

ABSTRACT

The Space Shuttle Columbia's catastrophic failure has been attributed to a piece of external fuel tank insulating SOFI (**S**pray **O**n **F**oam **I**nsulation) foam striking the leading edge of the left wing of the orbiter causing significant damage to some of the protecting heat tiles. The accident emphasizes the growing need to develop effective, robust and life-cycle oriented methods of nondestructive testing and evaluation (NDT&E) of complex conductor-backed insulating foam and protective acreage heat tiles used in the space shuttle fleet and in future multi-launch space vehicles. The insulating SOFI foam is constructed from closed-cell foam. In the microwave regime this foam is in the family of low permittivity and low loss dielectric materials. Near-field microwave and millimeter wave NDT methods were one of the techniques chosen for this purpose. To this end several flat and thick SOFI foam panels, two structurally complex panels similar to the external fuel tank and a "blind" panel were used in this investigation. Several anomalies such as voids and disbonds were embedded in these panels at various locations. The location and properties of the embedded anomalies in the "blind" panel were not disclosed to the investigating team prior to the investigation. Three frequency bands were used in this investigation covering a frequency range of 8-75 GHz. Moreover, the influence of signal polarization was also investigated. Overall the results of this investigation were very promising for detecting the presence of anomalies in different panels covered with relatively thick insulating SOFI foam. Different types of anomalies were detected in foam up to 9" thick. Many of the anomalies in the more complex panels were also detected. When investigating the blind panel no false positives were detected. Anomalies in between and underneath bolt heads were

not easily detected. This paper presents the results of this investigation along with a discussion of the capabilities of the method used.

Keywords: *microwaves, millimeter waves, near-field, insulating foam, disbond, void.*

INTRODUCTION

The Space Shuttle Columbia's catastrophic failure has been attributed to a piece of external fuel tank insulating SOFI (**S**pray **O**n **F**oam **I**nsulation) foam striking the leading edge of the left wing of the orbiter causing significant damage to some of the protecting heat tiles. According to the Columbia Accident Investigation Board (CAIB) report, the flyaway foam from the fuel tank was "the most probable cause" of the wing damage that brought down the space shuttle Columbia [1]. The accident emphasizes the growing need to develop effective, robust and life-cycle oriented methods of nondestructive testing and evaluation (NDT&E) of complex conductor-backed insulating foam and protective acreage heat tiles used in the space shuttle fleet and in future multi-launch space vehicles.

The insulating SOFI foam is constructed from closed-cell foam. In the microwave regime this foam is in the family of low permittivity and low loss dielectric materials. When applied to the external fuel tank the thickness of the foam can vary significantly from a few millimeters to tens of centimeters. The potential anomalies that may be present in the foam (e.g., air pockets, delamination and disbond) have very similar dielectric properties to the foam itself. Therefore, the dielectric contrast between the foam and a potential anomaly is very small. In addition, the structural geometry of the external fuel tank is very complex near the bipod and in the stringer regions. The combination of these restrictive factors significantly limits the utilization of many standard NDT methods for effective and robust inspection of the inner structural characteristics of the Space Shuttle's external tank insulating SOFI foam.

Subsequent to the Space Shuttle Columbia's catastrophic failure, NASA Marshall Space Flight Center embarked upon a program of evaluating all NDT methods suitable for inspecting the SOFI foam. Near-field microwave and millimeter wave NDT methods were one of the techniques chosen for this purpose [2-4].

Near-field microwave NDT&E methods have shown great promise for inspecting thick and multi layered (sandwich) dielectric composites for detecting anomalies such as void, disbond, delamination, impact damage, porosity variation, etc. [5-15]. One of the more attractive attributes of these methods is the fact that microwave and millimeter wave signals can easily

penetrate inside dielectric composites and interact with their inner structure. This is particularly relevant when inspecting low loss dielectric materials such as the SOFI insulating foam. In addition, microwave and millimeter wave systems designed and constructed for this purpose are small, low-powered (< 10 mW), handheld, portable, adaptable to commercial 2D scanners, fast, operator friendly (i.e., no microwave engineering skill requirements), low-cost and provide real-time data/image.

This paper presents the results of the microwave and millimeter wave NDT of the SOFI foam, and the results of a subsequent blind test on a relatively small panel similar in geometry and foam structure to a section of the external fuel tank. This panel was embedded with anomalies (e.g., voids and disbonds) of different sizes, shapes and locations unknown to the investigating team.

SAMPLE PREPARATION

An extensive set of measurements was performed on several SOFI foam panels similar in structure and properties to that used in the shuttle external fuel tank. The initial panels were constructed of flat and thick (up to 9" thick) SOFI foam backed by aluminum plates. Embedded in these panels were various inclusions such as small metallic and rubber washers. These initial panels were used to assess the basic capability of these microwave techniques for inspecting thick insulating SOFI foam. As the investigation progressed, panels with increasing geometrical complexity were investigated. During the latter part of the investigation more realistic panels, representing the structure of the Shuttle external fuel tank, were investigated. The embedded anomalies were designed to closely represent those that may be encountered in the external tank insulating SOFI foam. These anomalies included voids and disbonds of different sizes, and they were placed at different locations within a panel. A void was produced by hollowing out a cubical piece of foam prior to placing it in the desired location and spraying foam on it prior to completing the panel construction. A disbond was produced by cutting a thin squared shaped foam and adhering it to the foam by using a thin layer of adhesive prior to spaying it prior to completing the panel construction.

MEASUERMENT APPROACH

The panels were placed on a computer-controlled 2D scanning table and a microwave probe was held at a certain standoff distance above the panels [5]. Several laboratory-designed microwave reflectometers were used for inspecting these panels. The reflectometers either incorporated open-ended rectangular waveguide probes or small horn antennas. The horns provided for a certain degree of signal focusing resulting in increased spatial resolution. In this approach, an incident microwave signal, at a specific frequency, irradiates the panels. The incident signal is then partially reflected by the panel, and is subsequently picked up by the probe. The ratio of the reflected to the incident signal referenced at the probe aperture gives the effective reflection coefficient of the panel. This is a complex parameter whose phase and magnitude can be used to detect and evaluate the presence of an anomaly. The reflectometer output used here is then a voltage proportional to the phase and/or magnitude of the reflection coefficient. Subsequently, as the probe scans the panel, the probe output voltage is used to produce a raster scan or a 2D image of the panel. The measured voltages in this measured matrix are then normalized and assigned different grayscale levels producing a grayscale image, respectively. In this way, the grayscale levels in one image do not necessarily correspond to the same output voltage levels (e.g., colors) in another image. Therefore, in some cases when two images are to be compared, their matrices are first augmented, and subsequently the new matrix is normalized and a new image is produced. In this way the voltages associated with different regions of the original two images can be directly compared.

Anomalies such as air voids and disbonds are not expected to strongly scatter or reflect the incident microwave signal. Consequently, when a signal interacts with an anomaly and the reflected signal is picked up by the microwave probe, the signal phase variations due to the presence of the anomaly may be a stronger indication of the presence of the anomaly than the signal magnitude variations. Therefore, throughout this investigation, phase sensitive microwave reflectometer systems were utilized [5]. Four microwave frequency bands were considered and utilized in this investigation; namely, individual frequencies in X-band (8.2-12.4 GHz), K-band (18-26.5 GHz), Ka-band (26.5-40 GHz) and V-band (50-75 GHz).

RESULTS

As mentioned earlier, several initial flat panels were used to determine the basic effectiveness of these microwave measurements for inspecting thick insulation foam structures. The foam thickness in these panels varied from 6" to 9" and metallic and rubber washers were embedded inside the foam approximately 2" above the aluminum plate backing. Figure 1a shows the picture of a 9"-thick panel, while Figure 1b shows the X-band image of the embedded washer (dimensions are in mm). The image clearly shows the washer and provides a close estimate of its relative size (considering the distance between the probe and the washer).

Another 4"-thick flat panel was produced having a thin cork (~3/8" thick) substrate/base applied to the aluminum backing and several disbonds and air voids were embedded on and underneath the cork substrate. All anomalies were detected at K-band and Ka-band. Originally when a disbond was detected in this panel, an interesting "clover-like" pattern was detected in its image. Upon further discussions with those who produced this panel it became evident that the disbond was created by using a thin squared-shaped foam which was secured to the cork substrate using small daps of adhesive at each of its corners. The microwave image of this manufactured disbond at K-band is shown in Figure 2, which clearly shows the disbond and the "clover-like" pattern due to the individual daps of adhesive. The result was significant as it showed the relatively high spatial resolution that may be obtained using these microwave methods. It also indicated the presence of a thin air gap between the cork and the foam section, which is a "real" disbond (the region in the center of the "clover-like" pattern). Another interesting feature was also encountered when inspecting this panel. The microwave images of a set of four voids indicated them to be located at a different place and relative configuration than the schematic of the panel indicated. Once more, upon further discussions it became evident that the actual placing of the voids was not according to the original schematic, but was according to what was indicated by the microwave image.

A 2" inch-thick panel was investigated, at Ka-band and V-band, in which 40 embedded air voids existed. The schematic of the panel is shown in Figure 3a. The limited scan area associated with the scanning table could not accommodate scanning the entire panel at once. Consequently, several sections of this panel were individually scanned first, and then the resulting images were

augmented to produce an image corresponding to the entire panel. Figure 3b shows an image of this panel obtained at V-band. From this image, one can see that air voids as small as 0.25" in diameter were relatively easily detected throughout the panel thickness. Potentially, an additional indication such as an unintended rollover void, which was most likely produced during the manufacturing of the panel, was also detected as shown in the image. The outcome of this experiment and the resulting image confirms the potential of these microwave measurement for producing significant detail about the relative size and location of an anomaly in the SOFI foam. The different intensity levels associated with the air voids of similar size gives indication of the relative depth of the voids. In addition, this image revealed some features that are associated with the spraying process (the curved patches in the bottom right side of the image).

The panels investigated thus far did not include any complicated structural features in their conductor backing, and their foam thicknesses were relatively constant. The next experiment involved a panel containing similar structural features and complexity to that of the external fuel tank. Figure 4 shows a 3' by 3' panel, prior to spraying it with SOFI foam on it, showing various structural components such as four open-top stringers bolted to the metal backing, four bolts joining two vertical metal flanges producing a ridge of about 1" in width, and a relatively large flat area (i.e., approximately the top half of the panel). The approximate locations of various embedded air voids and disbonds are also shown in Figure 4. This panel was then spayed with SOFI foam in the same manner and geometry as the real respective section of the external fuel tank. Many of the embedded anomalies were detected and their microwave images were produced, with several of these examples discussed here. Figure 5 shows the image of the 3/4" corner void (to the left of the left most bolt) at K-band. The image clearly shows the void and its boundaries in the presence of the bolt. This image was minimally processed to remove the influence of changing SOFI foam thickness in this region. Figure 6a shows the 2" disbond in between the second and the third stringers, at K-band. The presence of the row of bolt heads on both sides of this anomaly is also shown in this image. To better demonstrate this, Figure 6b shows the image of a section of a stringer (devoid of anomalies) showing the rows of bolts on either sides of it.

Subsequent to demonstrating the capability of these microwave methods for detecting and evaluating anomalies in various locations within simple and thick SOFI foam panels and more typical and structurally complicated panels, a blind test was conducted. This test involved inspecting a section of a panel, similar in geometry to that shown in Figure 4, possessing three stringers. Additionally, several anomalies had been embedded in this panel. The locations of these anomalies were not revealed to the investigating team (e.g., a blind panel). The metal backing also included several equally spaced drilled holes around its edges. These holes are strong scatterers, however they are not anomalies for the purpose of this investigation. Figure 7 shows a picture of this panel with the stringers numbered as shown.

This panel was scanned (section by section) at K-band, Ka-band and some portions at V-band at two orthogonal polarizations. The images obtained from these sections where then patched together to produce an image of the entire panel. Figures 8a and 8b show the patched images of the panel at K-band using parallel and orthogonal polarizations, respectively. Parallel polarization refers to the case where the incident electric field vector is parallel to the long axes of the stringers, while orthogonal polarization refers to when the incident electric field vector is orthogonal to the axes of the stringers. These images show much detail about the internal structure of the panel as well as showing several of the "potential" embedded anomalies. Potential refers to the fact that these detected indications were to be later verified using destructive testing. Subsequently, the foam was destructively inspected for the presence of these "potential" anomalies.

It must be noted that structural features, whose primary axes are parallel to the incident wave polarization vector, are expected to be more clearly detected. This fact is evident in Figure 8a when considering the image from the stringers and the bolt heads. Both of these features have axes parallel to the incident electric field polarization vector and hence are clearly detected. The rings around the bolt heads are due to edge scattering form the bolts.

Both images clearly show the presence of the through holes around the bottom edge of the panel. The panel also possessed a natural and visible disbond at the bottom of the ramp adjacent to stringer #3. Figures 8a and 8b clearly show the presence of this disbond (when compared to the

same region near stringer #1). Figure 8a also shows three distinct indications of potential voids (labeled A-C). It is important to note that two of these potential voids are near strong scattering objects, namely a through hole and a bolt head, respectively. Nevertheless, their presence is clearly indicated in this image. To better illustrate the presence of potential void A, Figure 9 shows the region immediately surrounding this anomaly using parallel polarization. One can clearly see the indication associated with the presence of this potential void.

Stringer #3 opening region is clearly different than the same region for the other two stringers. Initially it was determined that there must be a void in the opening region of stringer #3. This decision was partially due to the fact that the other two stringer opening regions produced very similar images. To increase the level of confidence in associating a potential embedded void in this region, the image of the three stringer opening were also produced at Ka-band. Figures 10 shows the augmented images of these three regions, indicating a clear difference in the image obtained from stringer #3 opening region than the other two stringers. Consequently, the investigating team decided that stringer #3 opening region must have a potential void in it. It is very important to note that there are many stringers around the real external fuel tank. Consequently, images from many of these areas which can be compared and a decision about the presence of potential voids can be made with much higher levels of confidence and certainty on the real external tank. In this investigation we only had three such areas available and the decision to indicate a potential void in stringer #3 opening region was made based on the obtained images from these limited number of stringers.

Subsequently, the foam was destructively inspected for the presence of the potential anomalies. The "potential" voids (A-C) were verified to exist and be located where the microwave images indicated them to be. However, something interesting was discovered when inspecting the stringer opening regions. It turns out that two similar voids were embedded in the opening regions of stringers #1 and #2. All images from these two regions show extreme similarity corroborating the fact that these regions were indeed similar. However, an unintentional void was discovered in the stringer #3 opening region. All images produced from this region showed significant difference between it and the same regions in stringers #1 and #2. This finding is

very significant and clearly shows the potential applicability of this inspection method for evaluating the state of the external fuel tank SOFI foam.

DISCUSSION

Overall the results of this investigation were very promising for detecting the presence of anomalies in different panels covered with relatively thick insulating SOFI foam. Different types of anomalies were detected in foam up to 9" thick using microwave sources transmitting less than 10 mW of power. From the images obtained in this investigation, the capability of these microwave and millimeter wave methods for producing relatively high-resolution images of anomalies and the inner structure of the panels is clearly evident. When conducting these measurements it is very easy to manipulate the frequency of operation as shown in this paper, for obtaining more details about the inner structural characteristics of the tank. This is an important issue from a practical point of view since several systems operating at several frequency bands may be used to not only corroborate the inspection results at one band, but also to produce additional information about an anomaly (e.g., its size, depth within the foam, etc.). Furthermore, using two orthogonal signal polarizations a set of images can be produced that when studied together can provide more information than when a single polarization is used. Orthogonal polarization measurements can be easily accomplished by simply adjusting the relative orientation of the broad dimension of the open-ended waveguide probe or the horn antenna. More importantly, the images produced using these methods are self-explanatory and an operator can deduce much valuable information from the raw images. This feature makes these systems suitable for spot checking of critical region of the Space Shuttle.

Another significant issue is that no false positive indications were produced even in areas with complex geometry (e.g., stringers). Furthermore, an unintentionally manufactured void in the "blind" panel was detected. It is also important to note that due to the structural periodicity associated with the external tank, comparison of images obtained from similar areas can yield quick and useful information about the presence of a potential anomaly. This is important since it reduces the decision making time by an operator and provides for a degree of repeatability, redundancy and increased measurement robustness.

Anomalies under bolts and in between bolt heads were not satisfactorily detected. This is primarily due to the fact a metallic bolt masks any anomaly underneath in the former case, and strong scattering from bolt heads tends to mask indication of an anomaly in the latter case, respectively. In addition, primarily due to limitations in the scanning process, disbonds placed at the slanted sides of stringers were not detected either.

The majority of the images shown here were raw images to which no signal processing was applied. In some cases a row or a column of an image was subtracted from the rest of the image to reduce the influence of standoff distance or foam surface profile variations (i.e., slanted foam surface). There are many simple, fast and commercially available signal processing algorithms that can be incorporated into these microwave and millimeter wave NDT&E measurements to further improve the quality of the images. These algorithms may render enhanced images for obtaining information about the presence and properties of a potential anomaly.

The systems used here can be employed at various external tank construction stages such as when spraying the foam, after the foam has been sprayed and when all components have been attached. The ability to provide for this comprehensive *life-cycle* inspection is an important feature of these measurement methods and systems. The methodology outlined and used in this investigation can also be directly applied to other areas of the Space Shuttle that require comprehensive and periodic inspection such as the orbiter's acreage heat tiles for detecting impact damage and disbonds. The incorporation of higher resolution probes is expected to aid in detecting anomalies in highly scattering areas. Alternatively a lens-corrected horn antenna which provides narrow spot beams may also be used to inspect such areas [13]. If necessary, the depth of an anomaly can be evaluated using a calibration approach based on conducting a thorough electromagnetic simulation [6], or using a custom-made band-limited time-domain measurement setup.

The scanning systems used for most of this investigation were limited to scanning relatively small areas of the panels. Consequently, augmented or patched images, resulting in a larger image of the panels, were not always easy to interpret. For example, comparing this method to others, that were investigated for potential use on the space shuttle external tank, those with

larger scanning areas (i.e., 100 cm by 100 cm compared to 20 cm by 20 cm (used in this investigation) always produced easier to interpret images [3]. Since this is not a limitation of the inspection systems used in this investigation, it is expected that when they are incorporated into scanning systems capable of scanning larger areas easier to interpret images will result.

Finally, these measurement systems are relatively small, rugged, robust and readily portable. Further, these systems can be designed to be housed in operator-friendly packages suitable for handheld as well as automated measurements including those in space.

Acknowledgement: This work was supported by a grant from NASA George C. Marshall Space Flight Center, Huntsville, AL.

REFERENCES

1. Columbia Accident Investigation Board Report, NASA, August 2003.
2. Shrestha S., S. Kharkovsky, R. Zoughi, F.L. Hepburn and G. Workman, "Microwave Nondestructive Inspection of Thick Insulating Foam," Presented at *The American Society for Non-Destructive Testing (ASNT) Fall Conference and Quality Testing Show*, Pittsburgh, PA, 13-17 October 2003.
3. Davis C., F. Santos, "Shearography NDE of Space Launch Vehicles," Presented at *The American Society for Non-Destructive Testing (ASNT) Fall Conference and Quality Testing Show*, Pittsburgh, PA, 13-17 October 2003.
4. Madaras E., "Terahertz NDE for Inspection of Shuttle Foam," Presented at *The American Society for Non-Destructive Testing (ASNT) Fall Conference and Quality Testing Show*, Pittsburgh, PA, 13-17 October 2003.
5. Zoughi, R., *Microwave Non-Destructive Testing and Evaluation*, Kluwer Academic Publishers, The Netherlands, 2000.
6. Bakhtiari, S., S. Ganchev, N. Qaddoumi and R. Zoughi, "Microwave Non-Contact Examination of Disbond and Thickness Variation in Stratified Composite Media," *IEEE Transactions on Microwave Theory and Techniques*, vol. 42, no. 3, pp. 389-395, March 1994.
7. Qaddoumi, N., R. Zoughi, R. and G.W. Carriveau, "Microwave Detection and Depth Determination of Disbonds in Low-Permittivity and Low-Loss Thick Sandwich Composites," *Research in Nondestructive Evaluation*, vol. 8, no. 1, pp. 51-63. 1996.
8. Ganchev S., N. Qaddoumi, E. Ranu and R. Zoughi, "Microwave Detection Optimization of Disbond in Layered Dielectrics with Varying Thicknesses," *IEEE Transactions on Instrumentation and Measurement*, vol. 44, no. 2, pp. 326-328, April 1995.
9. Qaddoumi, N., T. Bigelow, R. Zoughi, L. Brown and M. Novack, "Reduction of Sensitivity to Surface Roughness and Slight Standoff Distance Variations in Microwave Inspection of Thick Composite Structures." *Materials Evaluation*, vol. 60, no. 2, pp. 165-170, February 2002.
10. Akothota, B., D. Hughes, R. Zoughi, J. Myers and A. Nanni, "Near-Field Microwave Detection of Disbond in Fiber Reinforced Polymer Composites Used for Strengthening

Concrete Structures and Disbond Repair Verification" *ASCE Journal of Materials in Civil Engineering*, (accepted for publication), 2004.

11. Zoughi, R. and S. Bakhtiari, "Microwave Nondestructive Detection and Evaluation of Disbonding and Delamination in Layered Dielectric Slabs," *IEEE Transactions on Instrumentation and Measurement*, vol. 39, no. 6, pp. 1059-1063, December 1990.
12. Bakhtiari, S. and R. Zoughi, "Microwave Nondestructive Detection and Evaluation of Void in Layered Dielectric Slabs," *Research in Nondestructive Evaluation*, vol. 2, no. 4, pp. 195-205, 1990.
13. Bakhtiari, S. N. Gopalsami, and A. C. Raptis, "Characterization of Delamination and Disbonding in Stratified Dielectric Composites by Millimeter Wave Imaging," *Materials Evaluation*, Vol. 53, No. 4, April 1995.
14. Gray, S., S. Ganchev, N. Qaddoumi, G. Beauregard, D. Radford and R. Zoughi, "Porosity Level Estimation in Polymer Composites Using Microwaves," *Materials Evaluation*, vol. 53, no. 3, pp. 404-408, March 1995.
15. Qaddoumi, N., S. Ganchev, G. Carriveau and R. Zoughi, "Microwave Imaging of Thick Composites with Defects," *Materials Evaluation*, vol. 53, no. 8, pp. 926-929, August 1995.

List of Figures

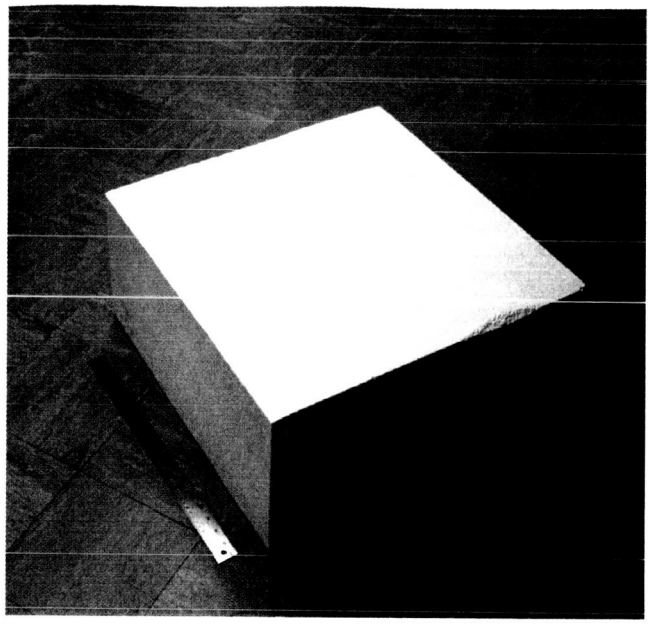

(a)

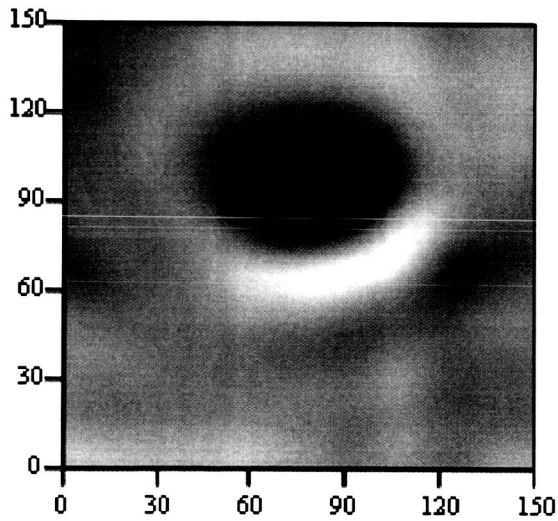

(b)

Figure 1

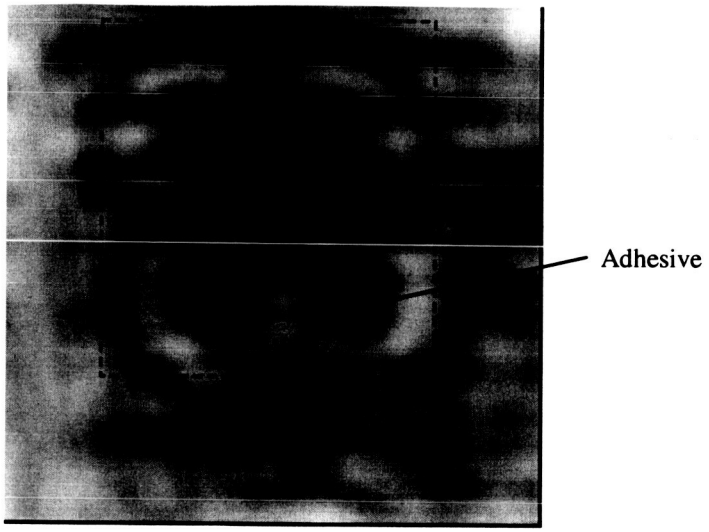

Figure 2

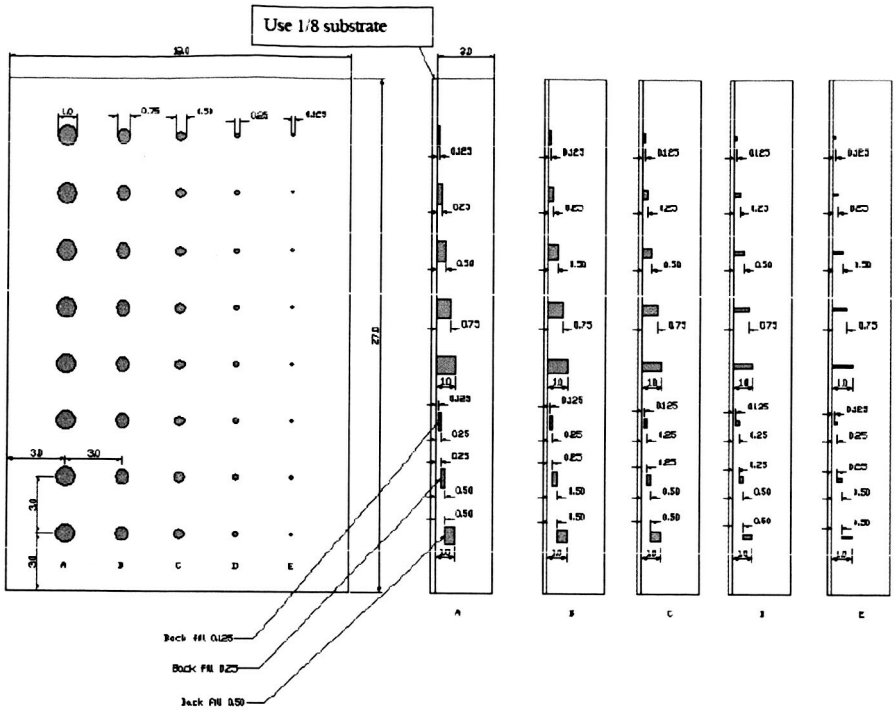

(a)

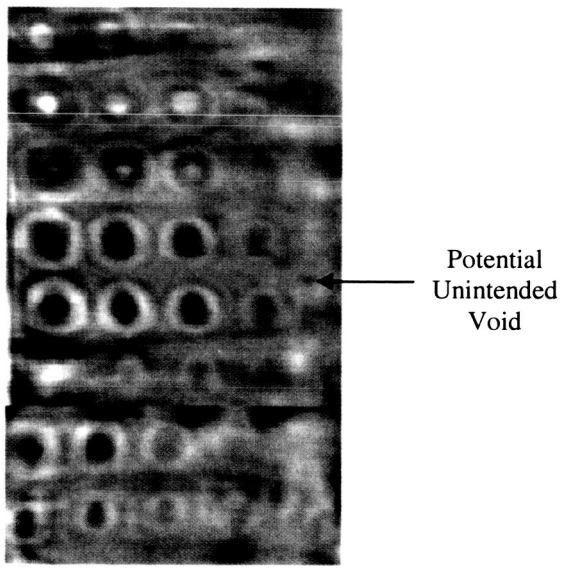

(b)

Figure 3

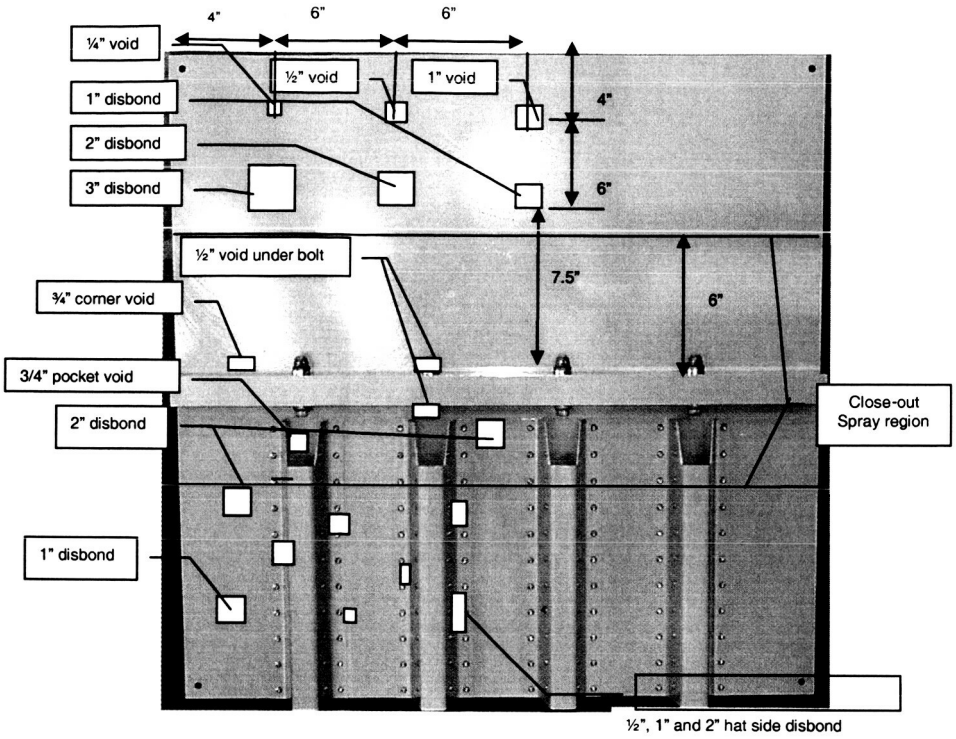
4"
6"
6"
¼" void
½" void
1" void
1" disbond
2" disbond
3" disbond
4"
6"
½" void under bolt
7.5"
6"
¾" corner void
3/4" pocket void
2" disbond
Close-out
Spray region
1" disbond
½", 1" and 2" hat side disbond

Figure 4

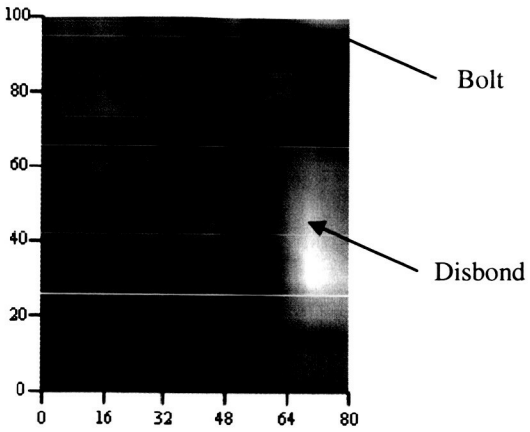

Figure 5

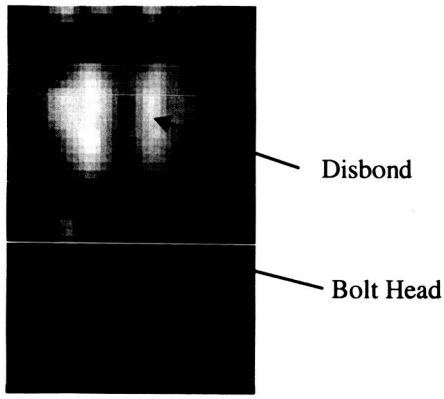

(a)

(b)

Figure 6

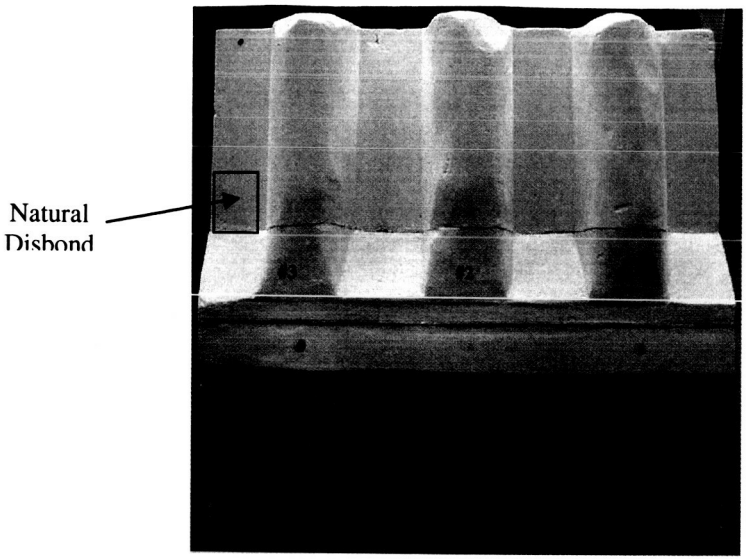

Figure 7

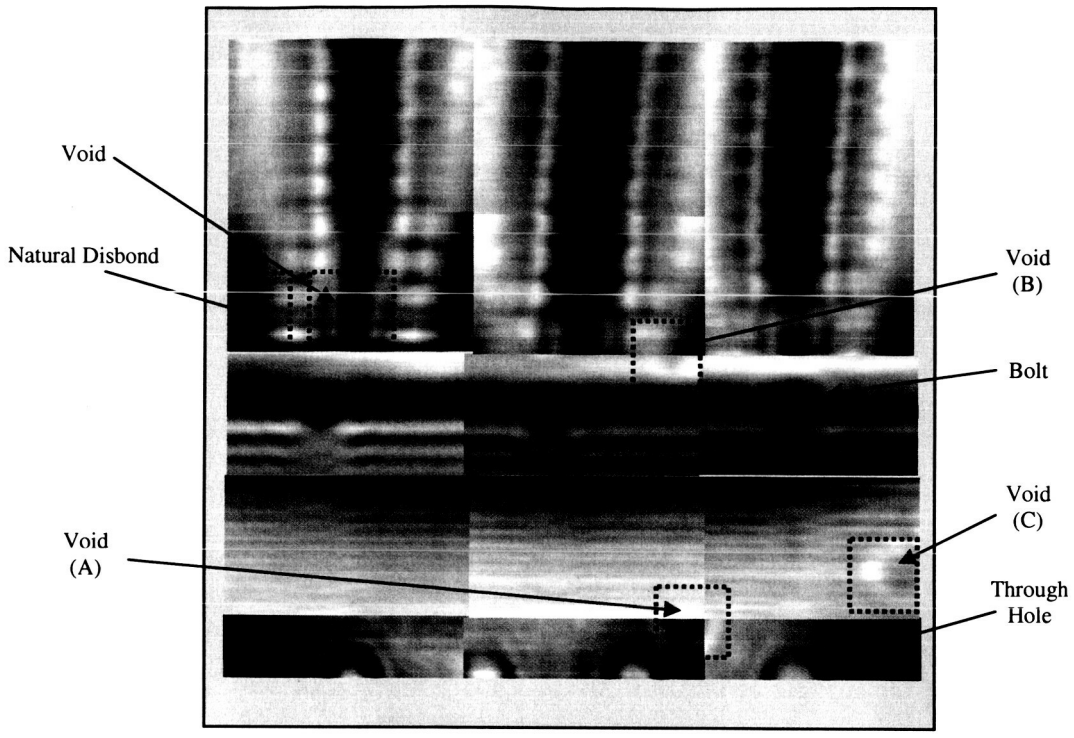
Void
Natural Disbond
Void
(B)
Bolt
Void
(C)
Void
(A)
Through
Hole

(a)

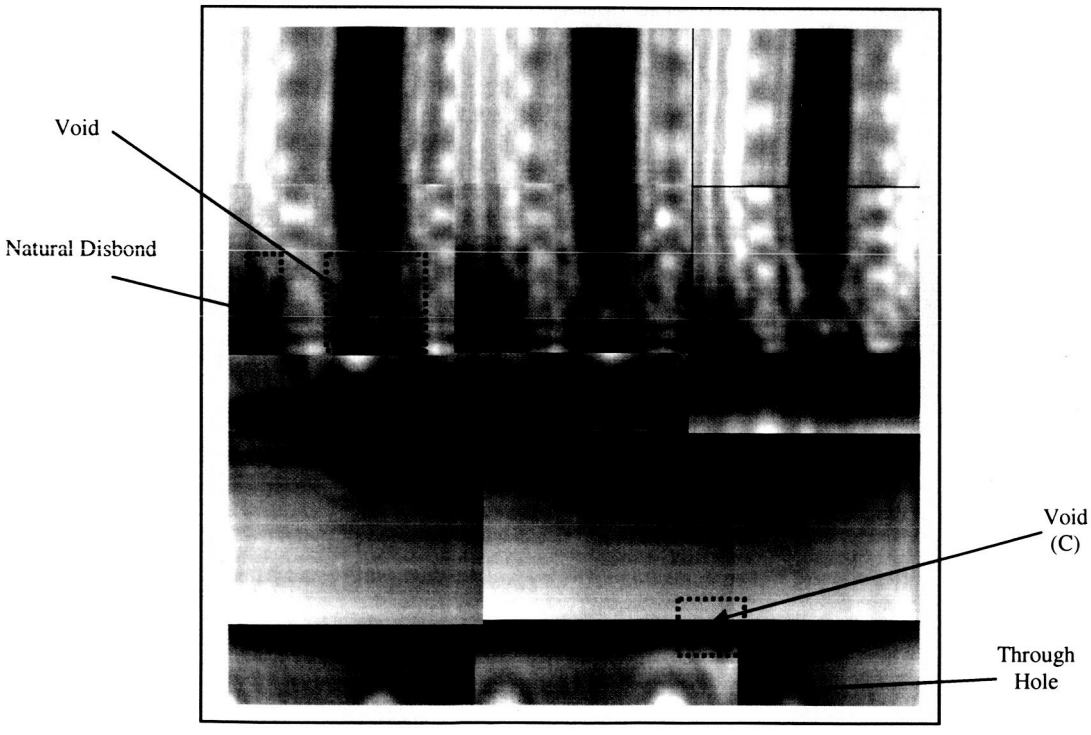
Void
Natural Disbond
Void
(C)
Through
Hole

Figure 8

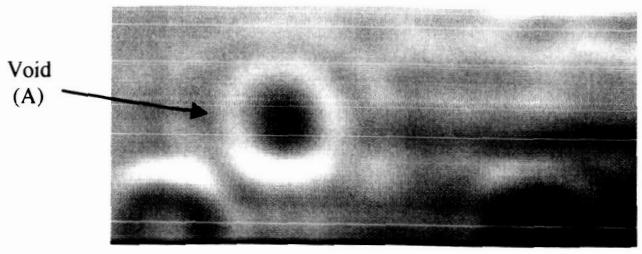

Figure 9

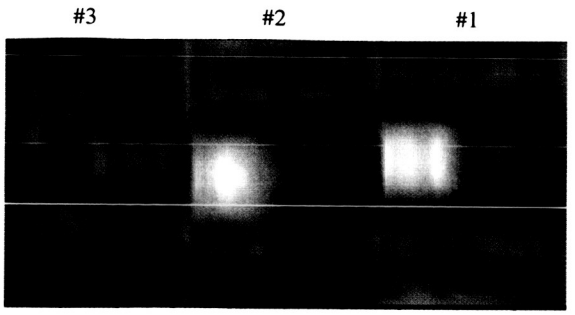

Figure 10